

# Adsorption of a Rake-Type Siloxane Surfactant onto Carbon Black Nanoparticles Dispersed in Aqueous Media

Yining Lin,<sup>†</sup> Thomas W. Smith,<sup>‡,§</sup> and Paschalis Alexandridis<sup>\*,†</sup>

Department of Chemical Engineering, University at Buffalo, The State University of New York, Buffalo, New York 14260-4200, and Xerox Corporation, 800 Phillips Road, Mailstop: 114-41D, Webster, New York 14580

Received November 14, 2001. In Final Form: May 23, 2002

The adsorption properties of a rake-type siloxane surfactant (consisting of a poly(dimethylsiloxane) backbone with grafted polyether) on carbon black (CB) nanoparticles have been investigated. The CB particles have fractal structure according to transmission electron microscopy and small-angle neutron scattering (SANS) data. Surface compositions, determined by X-ray photoelectron spectroscopy, indicate that the CB surface is partly oxidized, prove the adsorption of the siloxane surfactant onto the CB particles, and suggest that the surface coverage is incomplete. The adsorption obeys the Langmuir isotherm at low filtrate concentrations (below the critical micelle concentration, cmc). At higher filtrate concentrations, a sharp increase in the adsorbed amount is observed. The adsorbed layer thickness was determined by viscometry and dynamic light scattering. These two methods give good agreement on the adsorbed layer thickness (~30 nm) at surfactant concentrations above the cmc. This thickness is comparable to the hydrodynamic radius of the siloxane micelles in water. SANS experiments, performed under contrast matching conditions where either the CB particles or the siloxane surfactant was rendered "invisible", confirm that the adsorbed layer has structure and dimensions similar to those of siloxane surfactant micelles in aqueous solution in the absence of CB.

## Introduction

Pigments and other particles are widely used in the ink and coatings industry.<sup>1</sup> Surfactants are often added in these formulations, and they perform numerous functions acting as dispersants, wetting agents, emulsifiers, and antifoaming/defoaming agents.<sup>2</sup> The colloidal stability of systems containing dispersed particles depends largely on the amount and the hydrodynamic thickness of the adsorbed surfactant or polymer layer.<sup>3–8</sup>

Carbon black (CB) particles are essential ingredients in waterborne ink formulations where surfactants and polymers are also present. Surfactants are expected to adsorb onto CB particles by their hydrophobic parts and extend their hydrophilic parts into the aqueous medium, providing steric stabilization.<sup>9–11</sup> CB particles typically contain 90–99% elemental carbon, with oxygen and

hydrogen as the other major constituents. This composition renders CB particles strongly hydrophobic and prone to aggregation when dispersed in water. When CB is treated with oxidizing solution, surface oxides with acidic, for example, carboxylic, functional groups are formed. These groups render the carbon surface polar in character, and the CB particles become easier to disperse in aqueous media.<sup>12</sup> The structure of CB solids can be defined at three levels: primary particles (typically 10–100 nm in size) are fused together into aggregates (50–500 nm in size) that are packed into agglomerates (5 μm or larger in size). Electron microscopy has been used to characterize the morphology of CB in terms of bulkiness, anisotropy or shape factor, and, more recently, in terms of fractal dimension.<sup>13–16</sup> Small-angle scattering has been used to obtain surface fractal values for CB, various carbonaceous materials, and fumed silica.<sup>17–19</sup> The specific surface area

\* To whom correspondence should be addressed. E-mail: palexand@eng.buffalo.edu. Fax: (716) 645-3822.

<sup>†</sup> State University of New York.

<sup>‡</sup> Xerox Corp.

<sup>§</sup> Current address: Department of Chemistry, Rochester Institute of Technology, Rochester, NY 14623-5603.

(1) Carmine, J. L. The Use of Naphthenic Acid Ester as a Dispersing Agent in Aqueous Conductive Primers. *J. Coat. Technol.* **1994**, *66* (836), 93–98.

(2) Kang, H. R. Water-Based Ink-Jet Ink I. Formulation. *J. Imaging Sci.* **1991**, *35*, 179–188.

(3) Sato, T.; Ruch, R. *Stabilization of Colloid Dispersions by Polymer Adsorption*; Marcel Dekker: New York, 1980.

(4) Napper, D. H. *Polymeric Stabilization of Colloid Dispersions*; Academic Press: London, 1983.

(5) de Gennes, P. G. *Scaling Concepts in Polymer Physics*; Cornell University Press: Ithaca, NY, 1979.

(6) Scheutjens, J. M. H. M.; Fleer, G. J. Statistical Theory of the Adsorption of Interacting Chain Molecules. 1. Partition Function, Segment Density Distribution, and Adsorption Isotherms. *J. Phys. Chem.* **1979**, *83*, 1619–1635.

(7) Scheutjens, J. M. H. M.; Fleer, G. J. Statistical Theory of the Adsorption of Interacting Chain Molecules. 2. Train, Loop, and Tail Size Distribution. *J. Phys. Chem.* **1980**, *84*, 178–190.

(8) Shar, J. A.; Obey, T. M.; Cosgrove, T. Adsorption Studies of Polyethers: Part 1. Adsorption onto Hydrophobic Surfaces. *Colloids Surf., A* **1998**, *136*, 12–33.

(9) Stiffert, B.; Li, J. F. Adsorbed Polymer Layer Thickness Determination at the Solid–Liquid Interface by Different Techniques. *Colloids Surf.* **1992**, *62*, 307–314.

(10) Weiss, A.; Dingenouts, N.; Ballauff, M. Comparison of the Effective Radius of Sterically Stabilized Latex Particles Determined by Small-Angle X-ray Scattering and by Zero Shear Viscosity. *Langmuir* **1998**, *14*, 5083–5087.

(11) Andrew, D.; Joins, R.; Leary, B.; Boger, D. V. The Rheology of a Concentrated Colloidal Suspension of Hard Spheres. *J. Colloid Interface Sci.* **1991**, *147*, 479–495.

(12) Donnet, J. B.; Voet, A. *Carbon Black*; Marcel Dekker: New York, 1976.

(13) Sigerist, S.; Jullien, R.; Lahaye, J. Agglomeration of Solid Particles. *Cem. Concr. Compos.* **2001**, *23*, 153–156.

(14) Samson, R. J.; Mulholland, G. W.; Gentry, J. W. Structural Analysis of Soot Agglomerates. *Langmuir* **1988**, *3*, 272.

(15) Bourrat, X.; Oberlin, A. Mass Fractal Analysis of Conducting Carbon Black Morphology. *Carbon* **1988**, *26*, 100–103.

(16) Ehrburger-Dolle, F.; Tence, M. Determination of Fractal Dimension of Carbon Black Aggregates. *Carbon* **1990**, *28*, 448–452.

(17) Hjelm, R. P.; Wampler, W. A.; Seeger, P. A.; Gerspacher, M. The Microstructure and Morphology of Carbon Black: A Study Using Small Angle Neutron Scattering and Contrast Variation. *J. Mater. Res.* **1994**, *3210*–3222.

(18) Gerspacher, M.; O'Farrell, C. P. Carbon Black is a Fractal Object. An Advanced Look at an Important Filler. *Elastomerics* **1991**, *123* (4), 35–39.

(area/mass) of CB can also be estimated from small-angle scattering.<sup>20,21</sup>

Several authors<sup>22–24</sup> have studied the adsorption of ionic surfactants (such as sulfonate surfactants and cetyltrimethylammonium bromide (CTAB)) onto CB in aqueous solution. Ogura et al.<sup>23</sup> separated the suspension into filtrate and CB particles by ultracentrifugation and detected the sulfonate surfactant concentration in the filtrate by gel permeation chromatography. They found that a sufficient amount (>8%) of surfactant allows a high dispersion in the slurry, thus producing a pseudoplastic fluid with no yield values. Bele et al.<sup>24</sup> centrifuged the slurries and detected the supernatant concentration by polyelectrolyte titration. They found that after air-drying the amount of CTAB adsorbed from suspension does not change significantly. Langmuir type adsorption isotherms with a plateau region were found in the systems described above and in several other surfactant–particle systems. The plateau was reached in the vicinity of the critical micelle concentration (cmc) value (cmc for CTAB, 1.5 mmol/kg; for SDS, 30 mmol/L).<sup>24,25</sup> Small-angle neutron scattering (SANS) provided information on the coverage of the surfactants.<sup>26</sup> Garamus et al.<sup>26</sup> measured the micelle radius of the nonionic surfactant Triton-100 with and without CB particles. While the average radius of Triton-100 micelles was the same with or without the CB particles, the presence of CB particles shifted the cmc of the Triton X-100 to a lower value.

In the present study, we investigate the adsorption properties of a rake-type siloxane surfactant onto CB particles dispersed in water. This surfactant has a flexible poly(dimethylsiloxane) backbone rendered water-soluble via polyether (poly(ethylene oxide) (PEO)—poly(propylene oxide) (PPO)) grafts. We have recently studied the cmc and the structure of micelles formed by this surfactant.<sup>27–29</sup> The cmc of this surfactant is 0.05%, and the micelles formed in water are spherical at room temperature with a core diameter of approximately 15 nm.

The results presented here are organized in two main parts, one concerned with the CB particle structure and chemical composition and the other dealing with the amount and structure of the siloxane surfactant adsorbed

on CB dispersed in water. We characterized the structure of CB particles by transmission electron microscopy (TEM), scanning electron microscopy (SEM), and SANS. The surface chemical composition of the CB particles was determined by X-ray photoelectron spectroscopy (XPS). The adsorbed amount of siloxane on CB was obtained using dialysis; the surfactant concentration was determined by a colorimetric method. The adsorbed layer thickness was determined by viscometry and dynamic light scattering (DLS). The structure of the adsorbed layer was studied by SANS at conditions where the CB particles were “invisible”.

## Experimental Section

**Materials.** A CB aqueous suspension (15% CB) was supplied by Xerox Corp. The nominal diameter of the CB particles was reported in the range 100–120 nm. We provide in this work further evidence on the CB particle size and structure. The siloxane surfactant we studied here has the chemical formula MD<sub>70</sub>D<sub>5</sub>M (M: Me<sub>3</sub>SiO<sub>1/2</sub>–; D: –Me<sub>2</sub>SiO–; D': –Me(R)SiO–; R: polyether (PEO:900; PPO:300)) and MW = 11 500. This siloxane surfactant contains about 48% siloxane, 39% PEO, and 13% PPO. In this surfactant, 11% free polyether (MW = 1200, with 75% PEO and 25% PPO) existed due an excess polyether used in synthesis. Because of its relatively low molecular weight and high PEO content, the free polyether present in solution together with the siloxane surfactant is not expected to affect or mask the siloxane association properties. The stock solution was prepared by dissolving the surfactant in Milli-Q water (18 MΩ cm). D<sub>2</sub>O (used in SANS) was obtained from Cambridge Isotope Laboratories Inc. (Andover, MA). Ethyl acetate, cobalt nitrate, ammonium thiocyanate, and acetone were purchased from Sigma-Aldrich.

**SEM and TEM.** SEM experiments were carried out in a Hitachi S-450 scanning electron microscope. CB (0.3%) aqueous dispersions were deposited on glass slides and oven-dried overnight. TEM experiments were conducted with a JEOL model JEM2010 instrument. For these measurements, CB samples were diluted to 3.75 × 10<sup>–3</sup>% in methanol. A drop of the methanol suspension was placed on a microscope grid and was allowed to dry prior to the measurement.

**XPS.** The experiments were performed with SSIX-Probe (SSX-100) small spot XPS. The spectrometer used monochromatized Al Kα X-ray radiation. When the X-ray beam hits the sample, the atoms comprising the surface emit photoelectrons that can be counted by the detector and related to the atomic environment from which they originated in order to identify specific atoms. Dried CB particles and dried surfactant-coated CB powders (obtained from 0.5% siloxane surfactant in original solution containing 0.3% CB) were analyzed by XPS in order to determine their surface chemical composition.

Elemental analysis was achieved by selecting the carbon 1s line (285 eV) as a reference and then shifting the spectrum so that the reference peak was at the correct position. The binding energy range investigated was 0–1100 eV. Core electrons and Auger electrons of other elements were revealed on the spectrum. The peak areas were used for quantification of chemical composition. Around 20 eV of the C1s and O region was scanned at high resolution to give us the information about chemical shifts of the carbon (C1s) and oxygen (O1s) atoms. Common chemical shifts of C are unoxidized carbon (C1: C–C, C–H), carbon with one oxygen bond (C2: C–OH, C–O–C), carbon with two oxygen bonds (C3: O–C–O or C=O), and carbon with three oxygen bonds (C4: O=C–O).

**Adsorption Isotherm.** A CB (15%) aqueous dispersion was mixed with an aqueous siloxane surfactant solution (with surfactant concentration in the range 0.01–5%) so that the final concentration of CB particles equaled 0.3%, 1.5%, or 5%. The prepared slurries were rotated end-over-end for 24 h to ensure equilibrium adsorption. The suspensions were placed in Millipore Centricon Centrifugal filter tubes (MW cutoff, 100 000) and centrifuged at 3500g for 1 h. The slurries were then separated into retentate with CB particles and into clear filtrate (see schematic in Figure 1). The siloxane surfactant concentration of the filtrate solution was determined by the

(19) Reich, M. H.; Russo, S. P.; Snook, I. K.; Wagenfeld, H. K. Application of SAXS to Determine the Fractal Properties of Porous Carbon-Based Materials. *J. Colloid Interface Sci.* **1990**, *135*, 353–362.

(20) Beaucage, G. Small-Angle Scattering from Polymeric Mass Fractals of Arbitrary Mass-fractal Dimension. *J. Appl. Crystallogr.* **1996**, *29*, 134–146.

(21) Dekany, I.; Turi, L. Small-Angle X-ray Scattering of Hydrophobic and Hydrophilic SiO<sub>2</sub> Particles. *Colloids Surf., A* **1997**, *126*, 59–66.

(22) Ogura, T.; Tanoura, M.; Tsuchihara, K.; Hiraki, K. A. The Role of Surfactants in Achieving Highly Loaded Aqueous Suspensions of Organic Particles. *Bull. Chem. Soc. Jpn.* **1994**, *67*, 3143–3149.

(23) Ogura, T.; Tanoura, M.; Hiraki, K. A. Behavior of Surfactants in the Suspension of Coal Components. *Bull. Chem. Soc. Jpn.* **1993**, *66*, 1633–1639.

(24) Bele, M.; Kodre, A.; Arcon, I.; Grdadolnik, J.; Pejovnik, S.; Besenhard, J. O. Adsorption of Cetyltrimethylammonium Bromide onto CB from Aqueous Solution. *Carbon* **1998**, *36*, 1207–1212.

(25) Douillard, J. M.; Pougnet, S.; Faucompre, B.; Partyka, S. The Adsorption of Polyoxyethylenated Octyl and Nonyl Phenol Surfactants on CB and Sulfur from Aqueous Solutions. *J. Colloid Interface Sci.* **1992**, *154*, 11.

(26) Garamus, V. M.; Pedersen, J. S. A Small-angle Neutron Scattering of the Structure of Graphitized CB Aggregates in Triton X-100/Water Solutions. *Colloids Surf., A* **1992**, *132*, 203–212.

(27) Lin, Y.; Alexandridis, P. Microenvironment and Structure of Micelles Formed by a Polymeric Siloxane Surfactant in Aqueous Solutions. *Polym. Prepr. (Am. Chem. Soc., Div. Polym. Chem.)* **2001**, *42* (1), 229–230.

(28) Lin, Y.; Alexandridis, P. Self-Assembly of an Amphiphilic Siloxane Graft Copolymer in Water. Submitted for publication.

(29) Lin, Y.; Alexandridis, P. Cosolvent Effects on the Micellization of an Amphiphilic Siloxane Graft Copolymer in Aqueous Solutions. *Langmuir* **2002**, *18*, 4220–4231.

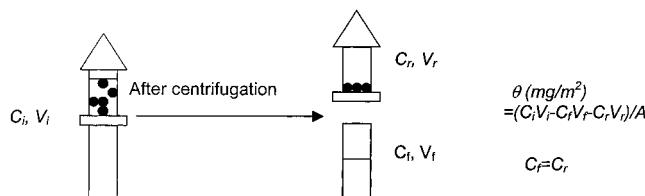


**Figure 1.** Schematic of the method for the determination of the adsorbed amount of siloxane surfactant on CB particles.

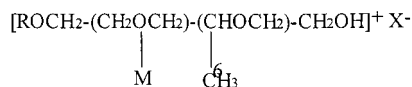
calibration curve obtained from a colorimetric method as described in the following section.

The adsorbed amount of siloxane surfactant on CB was calculated by mass balance. The adsorbed amount is the difference between the total amount of the surfactant initially added ( $C_i V_i$ ) and that present in the filtrate ( $C_f V_f$ ) and retentate ( $C_r V_r$ ) following adsorption (the retentate is assumed to have the same siloxane concentration as the filtrate). When calculating the siloxane surfactant concentrations for the adsorption isotherm, we took into account the free polyether present in solution. The adsorbed amount was calculated as follows:

$$m_2^s = (C_i V_i - C_f V_f - C_r V_r) / A \text{ (g/mL} \times \text{mL/m}^2\text{)}$$

where  $m_2^s$  is the adsorbed surfactant amount per unit area;  $C_i$ ,  $C_f$ , and  $C_r$  are the initial, filtrate, and retentate siloxane concentrations ( $C_f = C_r$ ), respectively;  $V_i$ ,  $V_f$ , and  $V_r$  are the initial, filtrate, and retentate volumes, respectively; and  $A$  is the surface area of carbon black particles.

**Colorimetric Method for the Determination of Siloxane Surfactant Concentration.** The colorimetric method that we used in order to measure the siloxane surfactant concentration is based on the formation of a colored complex between the PEO part of the siloxane surfactant and cobalt thiocyanate. The complex forms a precipitate that sediments upon centrifugation following the reaction of cobalt thiocyanate with the siloxane surfactant. The surfactant precipitate is dissolved in acetone, and the intensity of color is proportional to the amount of PEO present in the sample. The structure of the complex is postulated to be due to cobalt ion ( $M^+$ ) complexation with ether oxygen groups to form oxonium ion that reacts with a suitable anion ( $X^-$ ) such as thiocyanate. The postulated structure of the complex is shown below:<sup>30</sup>



Siloxane surfactant aqueous solution (400  $\mu\text{L}$ ) with a concentration ranging from 0.01 to 0.2%, 200  $\mu\text{L}$  of cobalt thiocyanate reagent, and 400  $\mu\text{L}$  of ethyl acetate were well mixed in a microcentrifuge tube (1.5 mL) and centrifuged for 15 min at 12 000*g*. The samples were shaken and then centrifuged for another 15 min. After centrifugation, the upper two layers were aspirated. Care was taken not to disturb the sediment. The sediment and the tube walls were washed with 400  $\mu\text{L}$  of ethyl acetate three times, and the aspirated ethyl acetate became colorless. The sediment was dissolved in 1.2 mL of acetone, and the absorbance was measured by a Beckman DU-70 UV-vis spectrophotometer at 331.5 nm. A calibration curve (Figure 2) was constructed, and the concentration of siloxane surfactant in the unknown samples was determined accordingly.

**Viscometry.** The adsorbed surfactant increases the effective radius of the particles and leads to a concomitant rise of the volume fraction of the particles in suspension.<sup>9-11</sup> An effective particle volume fraction  $\phi_{\text{eff}}$  can be defined through

$$\phi_{\text{eff}} = \phi_c \left(1 + \frac{\Delta}{a}\right)^3 = \phi_c k \quad (1)$$

(30) Ghebeh, M.; Corrigan, A. H.; Butler, M. Development of an Assay for the Measurement of the Surfactant Pluronic F-68 in Mammalian Cell Culture Medium. *Anal. Biochem.* **1998**, *262*, 39-44.

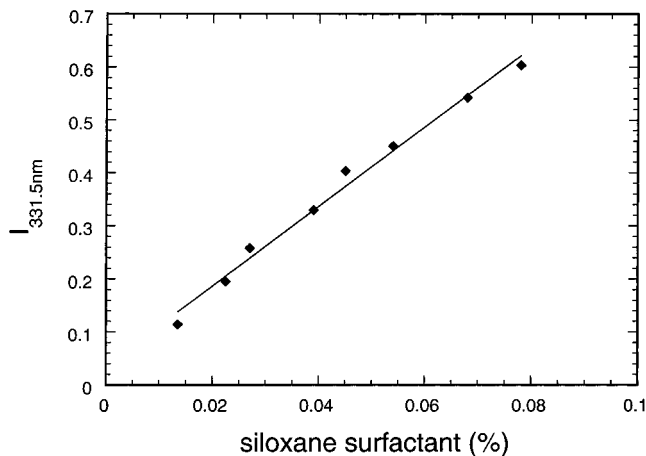


**Figure 2.** Calibration curve for the determination of siloxane surfactant concentration in water in the concentration range 0.01-0.1% siloxane.

where  $\phi_c$  and  $a$  denote the volume fraction and the radius of the plain particles and  $\Delta$  is the adsorbed layer thickness. In the dilute regime, the effective volume fraction of the particles can be determined from the relative viscosity of the suspension using the relationship

$$\frac{\eta_0}{\eta_s} = 1 + 2.5\phi_{\text{eff}} = 1 + 2.5k\phi_c \quad (2)$$

where  $\eta_0/\eta_s = \eta_r$  is the relative viscosity,  $\eta_0$  is the suspension viscosity, and  $\eta_s$  is the filtrate viscosity (i.e., the viscosity of the solution after removing the surfactant-coated particles). The factor 2.5 is the intrinsic viscosity for hard spheres (our CB particles are not exactly hard spheres, but eq 2 has been shown applicable to a variety of particles).  $k$  can be determined from the slope of the curve of the relative viscosity  $\eta_0/\eta_s$  plotted as a function of the volume fraction  $\phi_c$  of the particles. The adsorbed layer thickness  $\Delta$  can be calculated from the slope, and the curve should pass through  $\eta_r = 1$  when  $\phi_c = 0$ .

In some reports<sup>9,10,31</sup> that followed the above approach, the authors removed unadsorbed polymer by centrifugation or by reaction. The polymer (or surfactant) coated particles were then diluted to the required concentration, and the viscosities of the suspensions were measured. Because our CB particles would easily form aggregates during centrifugation, we followed the method described in ref 9. The viscosity of CB particles with and without surfactants in the volume fraction range of 0-2% was measured by a Cannon-Fenske viscometer at 24 °C. Figure 3 shows the filtrate concentration of siloxane surfactant corresponding to its initial concentration. The filtrate concentration of the siloxane surfactant at the end of the monolayer adsorption range and at the beginning of multilayer adsorption is 0.15% as determined from the adsorption isotherm for 0.3% and 1.5% CB suspensions (as discussed below, see Figure 4a). Figure 3 shows that at this filtrate concentration, the initial concentration of the surfactant is about 0.7%. Therefore, we choose this surfactant concentration to study the adsorbed layer thickness. The corresponding filtrate viscosity is 0.91 cSt. In this case, we assume that the adsorbed layer thickness does not change much with the CB amount in the suspension over the CB concentration range considered for the viscosity experiments.

**Dynamic Light Scattering.** Because the aqueous CB dispersions scatter light strongly, we must dilute them to a concentration at which the scattered light can be quantified. The selected CB concentration is  $3.75 \times 10^{-4}\%$ . The siloxane surfactant concentrations that we used to study the adsorbed layer thickness are 0.01% (below cmc) and 1% (above cmc). The measurements have been carried out by means of a Brookhaven BI-200SM goniometer equipped with a Lexel model 95 argon ion

(31) Neuhausler, S.; Richtering, W. Rheology and Diffusion in Concentrated Sterically Stabilized Polymer Dispersions. *Colloids Surf., A* **1995**, *97*, 39-51.



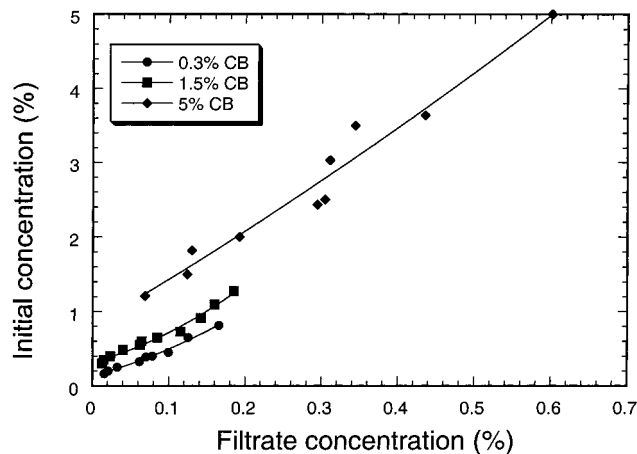


**Figure 3.** Initial concentration of siloxane surfactant added plotted vs the siloxane concentration in the filtrate following adsorption on CB.

laser as a light source. The detection angle was  $90^\circ$ . The wavelength of the laser light was 514 nm. The temperature was set at  $24^\circ\text{C}$ . The scattered intensity is recorded by means of a multichannel digital correlator and converted to the correlation function. In our study, the electric field correlation function  $|g^{(1)}(\tau)|$  was analyzed by the exponential sampling (EXPSAM) method, yielding information on the distribution function of  $\Gamma$  from:

$$|g^{(1)}(\tau)| = \int G(\Gamma) \exp(-\Gamma\tau) d\Gamma$$

$$\bar{\Gamma} = \int \Gamma G(\Gamma) d\Gamma$$

$G(\Gamma)$  can be used to determine an average apparent (or translational) diffusion coefficient  $D_{\text{app}} = \Gamma/q^2$  where  $q = (4\pi n/\lambda) \sin(\theta/2)$  is the magnitude of the scattering wave vector. The apparent hydrodynamic radius  $R_h$  is related to  $D_{\text{app}}$  via the Stokes–Einstein equation:

$$D_{\text{app}} = kT/6\pi\eta R_h \quad (3)$$

where  $k$  is the Boltzmann constant,  $T$  is the absolute temperature, and  $\eta$  is the viscosity of the solvent. To better visualize and quantify the measured micelle diameter distribution data and given that the Gaussian (bell-shaped) curve can describe well the micelle size distribution,<sup>40</sup> the size distribution data obtained from EXPSAM were fitted by Gaussian curves.<sup>29</sup>

**Small-Angle Neutron Scattering.** SANS measurements were performed at the National Institute of Standards and Technology (NIST) Center for Neutron Research, beam guide NG3. The neutron wavelength used was  $\lambda = 0.6$  nm. The sample to detector distance was 260.0 and 1300.0 cm. The resolution ( $\Delta q/q$ ) was about 0.15. The angular distribution of the scattered neutrons was recorded in a two-dimensional detector; the radial average was subsequently obtained and used for data analysis. The samples were placed in 1 mm path length stopper “banjo” quartz cells, and scattering data were recorded. Adequate time was allotted for thermal and kinetic equilibrium. Scattering intensities from the samples were corrected for detector background, empty cell scattering, and sample transmission using standard procedures.<sup>32–34</sup> The resulting corrected intensities were normalized to absolute cross section units.

Experiments of 0.3% CB in water with and without 1% siloxane were performed at  $25^\circ\text{C}$ . Two contrasts were used to study the

(32) Yang, L.; Alexandridis, P.; Steytler, D. C.; Kositzka, M. J.; Holzwarth, J. F. SANS Investigation of the Temperature-Dependent Aggregation Behavior of the Block Copolymer Pluronic L64 in Aqueous Solution. *Langmuir* **2000**, *16*, 8555–8561.

(33) Alexandridis, P.; Yang, L. Micellization of Polyoxyalkylene Block Copolymers in Formamide. *Macromolecules* **2000**, *33*, 3382–3391.

(34) Alexandridis, P.; Yang, L. SANS Investigation of Polyether Block Copolymer Micelle Structure in Mixed Solvents of Water and Formamide, Ethanol, or Glycerol. *Macromolecules* **2000**, *33*, 5574–5587.

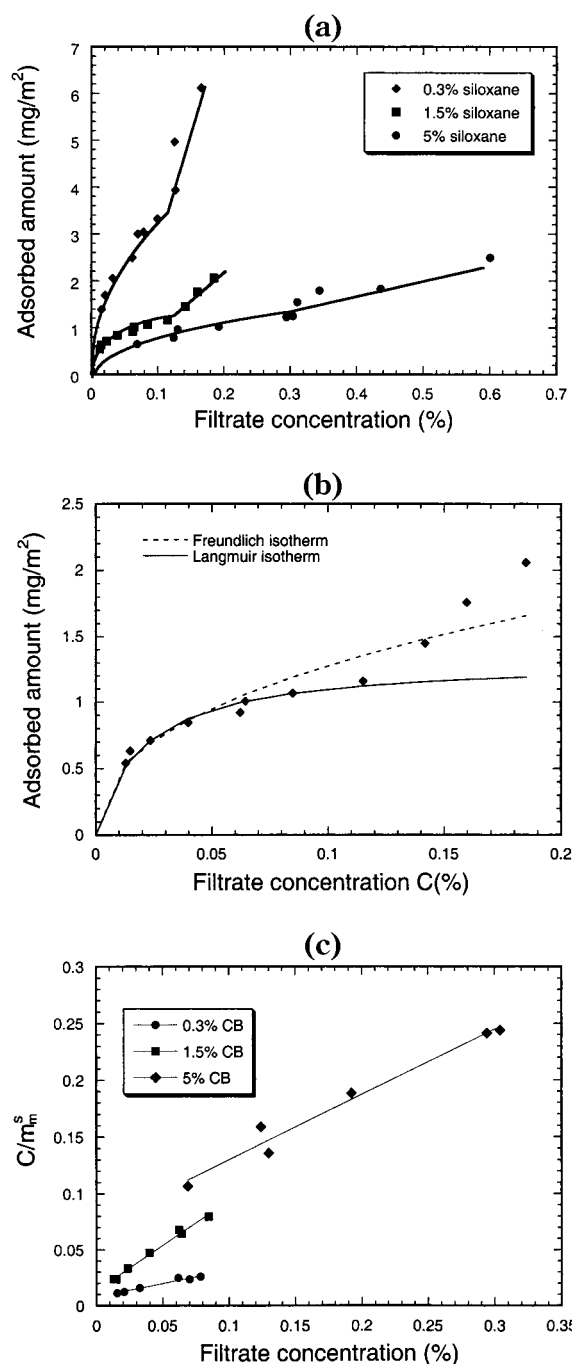


**Figure 4.** (a) Adsorption isotherm of siloxane surfactants onto CB particles of different concentrations. The adsorption follows the Langmuir isotherm at low filtrate concentrations and corresponds to monolayer adsorption. For 0.3% and 1.5% CB suspensions, the monolayer adsorption stops at about 0.15% siloxane, which is close to the cmc of the siloxane surfactant in water (0.05%). For 5% CB, the monolayer adsorption stops at 0.3%. Above these filtrate concentrations, a rapid increase in adsorbed amount is observed. (b) Two adsorption isotherm equations, the Langmuir and Freundlich isotherm, are used to fit the adsorption data of siloxane onto 1.5% CB. (c) Langmuir isotherm parameter determination.  $C_2/m_2^2$  vs  $C_1$  gives a straight line for all three CB concentrations, indicating that the adsorption follows Langmuir isotherm behavior at low filtrate concentrations. The parameters obtained from the fit are listed in Table 3.

structure of CB and of adsorbed siloxane. If we match the scattering length density (SLD) of the aqueous solvent using an appropriate mixture of  $\text{D}_2\text{O}$  and  $\text{H}_2\text{O}$ , we can detect the CB structure. On the other hand, if we match the SLD of the aqueous solvent with that of the CB, we can detect the structure of the

siloxane surfactant. The scattering length densities of CB and siloxane are  $6.5 \times 10^{10}$  and  $0.658 \times 10^{10} \text{ cm}^{-2}$ , respectively. We could eliminate the scattering contribution from CB at 100% D<sub>2</sub>O (SLD =  $6.33 \times 10^{10} \text{ cm}^{-2}$ ) and the scattering contributions of the siloxane surfactants at 87% H<sub>2</sub>O + 13% D<sub>2</sub>O solvent.

**SANS Data Analysis: Micelles.** The absolute SANS intensity can be expressed as a product of  $P(q)$  which is related to the form factor and the structure factor  $S(q)$ :<sup>32–34</sup>

$$I(q) = NP(q)S(q) \quad (4)$$

where  $N$  is the number density of the scattered particles, in our case micelles, which depends on the surfactant concentration and the association number of micelles. The particle form factor  $f(q)$  can be related to  $P(q)$  by the following expression:

$$P(q) = [V_p(\rho_p - \rho_s)f(q)]^2 \quad (5)$$

where  $V_p$  is the micelle particle volume, and  $\rho_p$  and  $\rho_s$  are the mean SLDs of the micelle particles and solvent, respectively. The form factor  $f(q)$ , which takes into account the intramicelle structure, depends on the shape of the colloidal particle. The hard-sphere form factor that describes a dense spherical particle with radius  $R$  can be calculated as

$$f(q) = 3[\sin(qR) - qR \cos(qR)]/(qR)^3 \quad (6)$$

In fitting the hard-sphere model to the scattering data, we view the micelle particles as consisting of a relatively “dry” core (composed of siloxane and PPO segments with little or no solvent present) and a relatively hydrated corona consisting of solvated PEO segments (PPO segments are relatively polar, but under the conditions of our experiments, they are more likely to participate in the micelle core than in the hydrated corona). When the siloxane surfactant solutions are prepared in D<sub>2</sub>O, then the contrast between the micelle core, with low SLD ( $\rho_{\text{siloxane}} = 6.58 \times 10^{-8} \text{ \AA}^{-2}$  and  $\rho_{\text{PPO}} = 3.25 \times 10^{-7} \text{ \AA}^{-2}$ ), and the solvent, with high SLD ( $\rho_{\text{D}_2\text{O}} = 6.33 \times 10^{-6} \text{ \AA}^{-2}$ ), is strong, but the contrast between the hydrated corona and the solvent is weak. Therefore,  $P(q)$  mainly depends on the hydrophobic micelle core, and the radius  $R$  obtained from the hard-sphere form factor corresponds to the micelle core radius (whereas the radius obtained from DLS reflects also the hydrated micelle corona). For a dilute solution, the structure factor is close to unity. With an increase in the surfactant concentration, a correlation peak will arise due to the intermicellar structure factor. In our data, we did not observe such a peak and therefore we consider  $S(q) = 1$ . We thus fit the 1% siloxane data using the hard-sphere form factor; there is only one parameter ( $R$ ) in fitting these data.

**SANS Data Analysis: CB Particles.** Under a mass-fractal model, the fractal dimension  $d_f$  describes the geometry of many random objects and scaling laws in small-angle scattering. The fractal dimension  $d_f$  is defined by

$$M(R) \propto R^{d_f}$$

where  $M$  is the mass of material contained in a sphere of radius  $R$  centered at an arbitrary point on the object. The fractal dimension can be obtained experimentally from SANS measurements and is determined from the negative slope of  $\log(\text{scattering intensity})$  versus  $\log(\text{scattering vector } q)$  in a power-law regime.

We use the unified equation developed by Beaucage et al.<sup>20,35</sup> to describe the limits to mass-fractal scaling at the aggregate radius of gyration  $R_{g2}$  and the primary particle radius of gyration  $R_{g1}$ . The unified equation under mass-fractal constraints is further constrained by assuming spherical primary particles. The unified approach breaks a complex scattering pattern into structural levels, each of which contains a Guinier regime reflecting the  $R_g$ , and particle contrast followed by a power-law regime which describes the type of structures to which the Guinier regime pertains. Each structural level is described, in the unified approach, by four generic parameters, a constant  $G$ , the radius

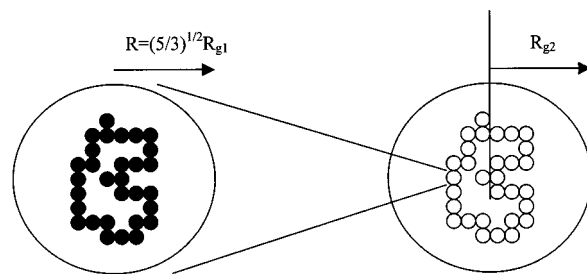


**Figure 5.** Schematic of the mass-fractal structure of CB particles.  $R_{g1}$  (from primary particles) and  $R_{g2}$  (from the cluster) are indicated.

of gyration  $R_g$ , the power-law prefactor  $B$ , and the power-law slope  $P$ . The scattering intensity in our data can be fitted by

$$I(q) = G_1 \exp(-q^2 R_{g1}^2/3) + B_1(1/q_1^*)^P + G_2 \exp(-q^2 R_{g2}^2/3) + B_2 \exp(-q^2 R_{g1}^2/3)(1/q_2^*)^d \quad (7)$$

where subscript 1 denotes the low- $q$  region (surface fractal and primary particles) and subscript 2 denotes the intermediate- $q$  region (mass-fractal region and composite). The radius of gyration,  $R_{g2}$ , for a mass fractal with mass-fractal dimension  $d_f$  and degree of aggregation  $z$  is given by

$$R_{g2} = \{b^2 z^{2/d_f} / [(1 + 2/d_f)(2 + 2/d_f)]\}^{1/2} \quad (8)$$

where  $b$  is the primary particle diameter, and  $b = 2R$ . Assuming CB has spherical primary particles, then  $R = (5/3)^{1/2} R_{g1}$ . The power-law prefactor  $B_2$  for mass-fractal aggregates is given by

$$B_2 = (G_2 d_f / R_{g2}^{d_f}) \Gamma(d_f/2) \quad (9)$$

where  $\Gamma$  is the gamma function. A mass fractal with spherical primary particles is described by four parameters under this model:  $z$ ,  $R_{g1}$ ,  $d_f$ , and  $G_1$ . The mass-fractal structure of CB particles is shown schematically in Figure 5.

**Specific Surface Area Estimation by SANS.** The surface area of CB can also be determined for the mass-fractal scaling regime of the small-angle scattering pattern. To calculate the surface area, the volume of the substructural unit ( $V_{pp}$ ) needs to be determined from the Porod invariant,  $Q$ , and the Guinier prefactor,  $G_1$ :

$$Q = \int_0^\infty I(q) q^2 dq = 2\pi^2 G_1 / V_{pp} \quad (10)$$

$I(q)'$  is given by the last two terms of eq 7.

For spherical primary particles, the surface area per primary aggregate  $S_{pp}$  can be estimated by

$$S_{pp} = K_{\text{sph}} R_{g2}^{d_f} R^{2-d_f}$$

where  $K_{\text{sph}} = 4\pi 2^{-d_f} (1 + 2/d_f)^{d_f/2} (2 + 2/d_f)^{d_f/2}$ . The specific area  $S$  can be obtained by taking the density  $\rho$  of the carbon black to be  $2 \text{ g/cm}^3$ .<sup>12</sup>

$$S = S_{pp} / \rho z V_{pp} \quad (11)$$

## Results and Discussion

**XPS.** XPS analysis examines only the top 2–10 nm of the CB surface. The XPS spectra of elemental analysis of dried CB particles and dried surfactant-coated CB particles are shown in Figure 6a,b. These figures show the peaks corresponding to the elements that are detected on the surface of the dried CB powders. Table 1 summarizes the quantified atomic percent concentrations at the surface. The fine features of carbon shifts associated with oxide bonding state are shown in Figure 7a,b. The relative contents of chemical shifts are listed in Table 2.

(35) Beaucage, G.; Schaefer, D. W. Structural Studies of Complex Systems Using Small-Angle Scattering: Unified Guinier/Power-Law Approach. *J. Non-Cryst. Solids* **1994**, *172*, 797–805.

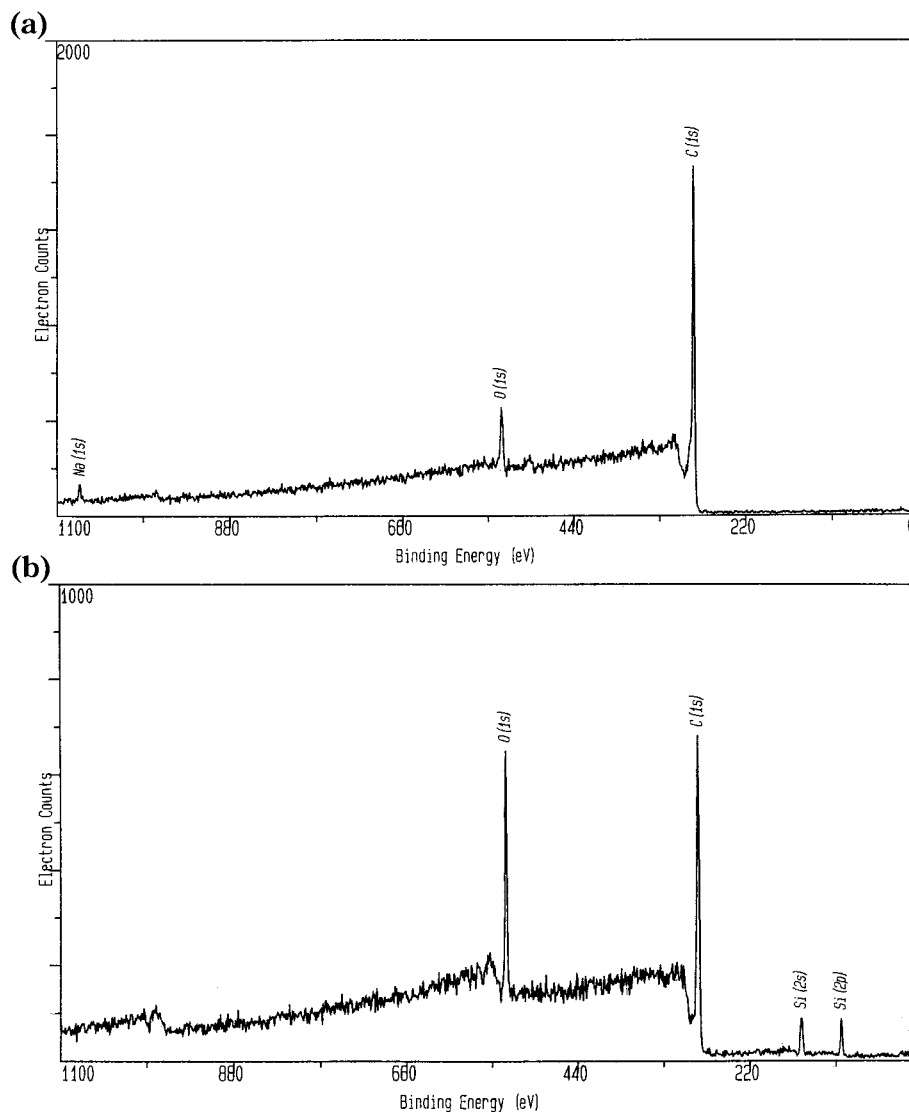


**Figure 6.** ESCA (electron spectroscopy for chemical analysis) spectra of the element compositions from the CB surface. The surface compositions of (a) plain CB particles and (b) CB particles after adsorbing siloxane surfactant are shown. Following the adsorption of the siloxane surfactant, the element Si appears in the spectra and the amount of O increases.

**Table 1. Atomic Percent Concentration at the Surface of CB Particles**

element	CB	CB with adsorbed siloxane
C	87.2	68
O	10.6	25.3
Si		6.2
Na	2	0.5
S	0.1	

**Table 2. Chemical Shifts of C1s and O1s at the Surface of CB Particles**

		CB (%)	siloxane-coated CB (%)
C1s	CC or CH <sub>2</sub>	93.4	62.5
	OC=O	6.6	
	CO		35.4
	differential charging		2.1
O1s	C=O or Na <sub>2</sub> S <sub>2</sub> O <sub>3</sub>	53.8	?
	CO or water	43.2	?

From Tables 1 and 2, we see that the atomic percent concentration at the surface of CB particles without added surfactant was 87.2% C, 10.6% O, 2% Na, and 0.1% S. The relative amount of C1s in the unoxidized state (C–C) is 93.4% and that of O–C=O is 6.6%. The relative amount of O1s associated with C=O is 56.8% and that with C–O or H<sub>2</sub>O is 43.2%. The presence of sodium element may be

due to contamination, counterions, or other additives. From the chemical shift data in Table 2, 6.6% of carbon in the form O–C=O is present on the surface of the CB. This indicates that the surface of CB particles without added siloxane surfactant is possibly oxidized in small portion with COO<sup>−</sup> groups and Na<sup>+</sup> as counterions. Note that the total amount of carbon forming O–C=O bonds is 6.6% out of 87.2% carbon, which equals 5.7% of O–C=O carbon. The oxygen associated with O–C=O bonding is 11.4% (2 × 5.7%), which is close to the value (obtained independently) of oxygen on the surface (10.6%). This good agreement supports the presence of COO<sup>−</sup> on the surface. The water contact angle is about 22° for the CB particles (as measured by a Rame-Hart model 100-10 contact angle goniometer), and this can be due to the polar COO<sup>−</sup> and Na<sup>+</sup> present on the CB particle surface. To measure the contact angle, these CB particle dispersions were deposited on glass slides and left to dry in the oven for 1 day. The contact angle value is close to that observed on a hydrophilic co-poly(ethylene oxide, propylene oxide) surface.<sup>41</sup>

The atomic percent concentration at the surface of the siloxane surfactant coated CB particles was 68% C, 25.3% O, 6.2% Si, and 0.5% Na. From Table 2, the relative amount

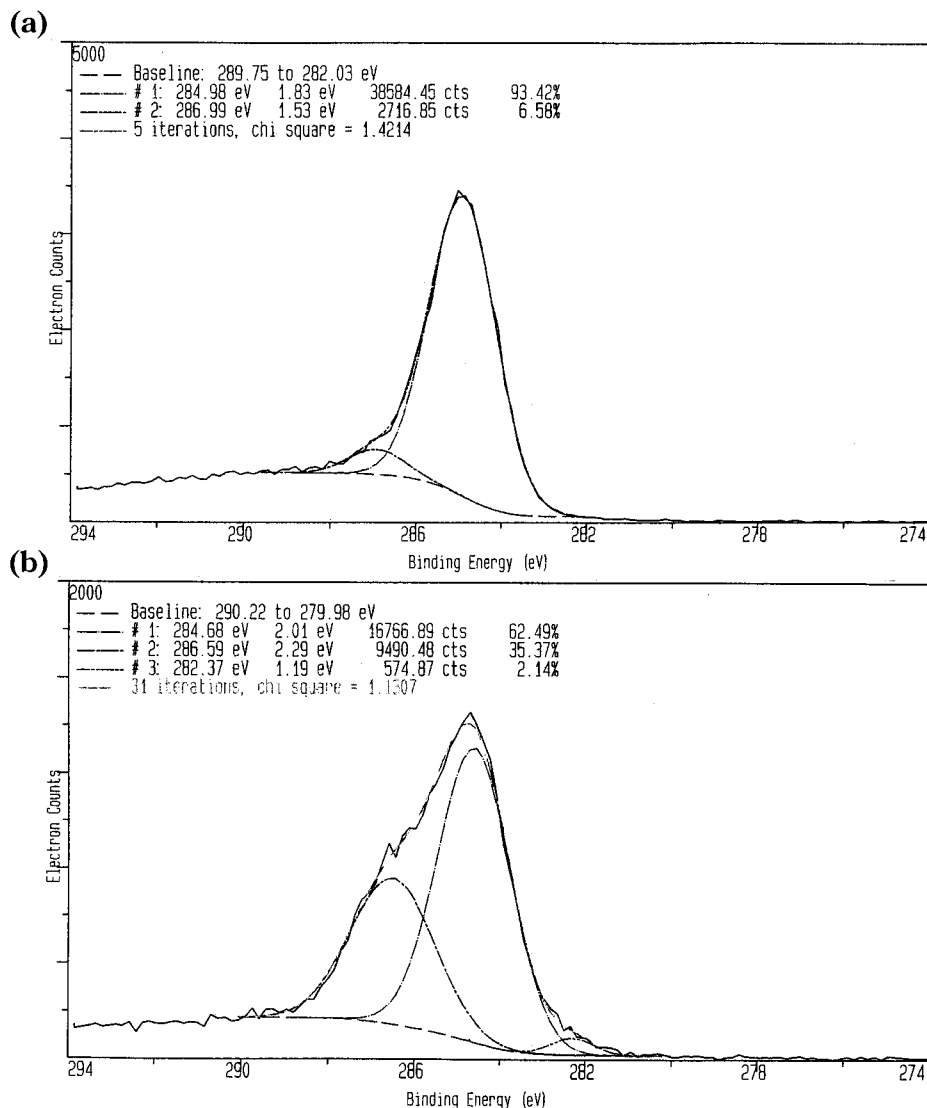


**Figure 7.** The deconvolution of the carbon element spectra shown in Figure 6. The spectra of the oxidation state of the C element for (a) plain CB and (b) CB particles after the adsorption of siloxane surfactant are shown. The atomic percentage of the C–C group decreases and C–O appears, proving the presence of siloxane on the particle surfaces.

of C1s in the unoxidized state is 62.5%, in C–O bonding is 35.4%, and in differential charging (where the sample surface is not homogeneous and some portion of the surface has more charges than the rest) is 2.1%. O1s can be related to the following possible states: C–O, C=O, and organic Si compound (Si–O). The peaks that correspond to these states overlap, and thus it is not easy to decouple their relative contributions.

CB particles with adsorbed siloxane surfactants increased the silicon concentration at the surface from 0 to 6.2% and the oxygen concentration from 10.6% to 25.3%. The carbon concentration decreased from 87.2% to 68%. The siloxane surfactant has a nominal composition of about 10 atomic % silicon, 30 atomic % oxygen, and 60 atomic % carbon (note that the hydrogen atoms cannot be discerned by XPS because their binding energy is too high, so we do not take them into account in the elemental composition). Theoretically, a CB particle has 100 atomic % carbon. Thus, the increase in silicon and oxygen concentrations as well as the decrease in carbon concentration observed in the CB powders containing the siloxane surfactant is consistent with the presence of the siloxane surfactant on the surface. Although the changes in atomic concentration were in the direction expected for the adsorption of the siloxane surfactant, the ratio of the

silicon, oxygen, and carbon determined from XPS is not 1:3:6 which would correspond to the siloxane surfactant; instead it is 1:3.9:10.5. There is still more oxygen and much more carbon which does not originate from the siloxane surfactant. This indicates that the surface coverage by the siloxane surfactant was incomplete. If we subtract the carbon and oxygen atomic concentration that should originate from the siloxane surfactant, the ratio of C/O remaining is 5. This is lower than the C/O ratio at the CB surface when no surfactant was added (8.2). It is possible that the oxidized parts on the CB particle surfaces are not covered by the surfactants.

The high-resolution C1s spectra showed some differential charging for the siloxane surfactant coated surfaces. After deconvoluting the O1s peaks, we find that the oxygen can be in different states. Some O–C=O bonds are possibly on the surface, which is not shown in Table 2. We believe that most oxygen comes from polyether present in the siloxane surfactants, which increased the percent of ether carbon from 0 to about 35.4%, while CH<sub>2</sub> or C–C bonding decreased from 93.4% to 62.5%. This is in agreement with both siloxane and graft polyether chains being located on the CB surface following drying. The ratio C–O/CH<sub>2</sub> of CB with adsorbed siloxane surfactant layers as determined from our experiments is 0.56. In



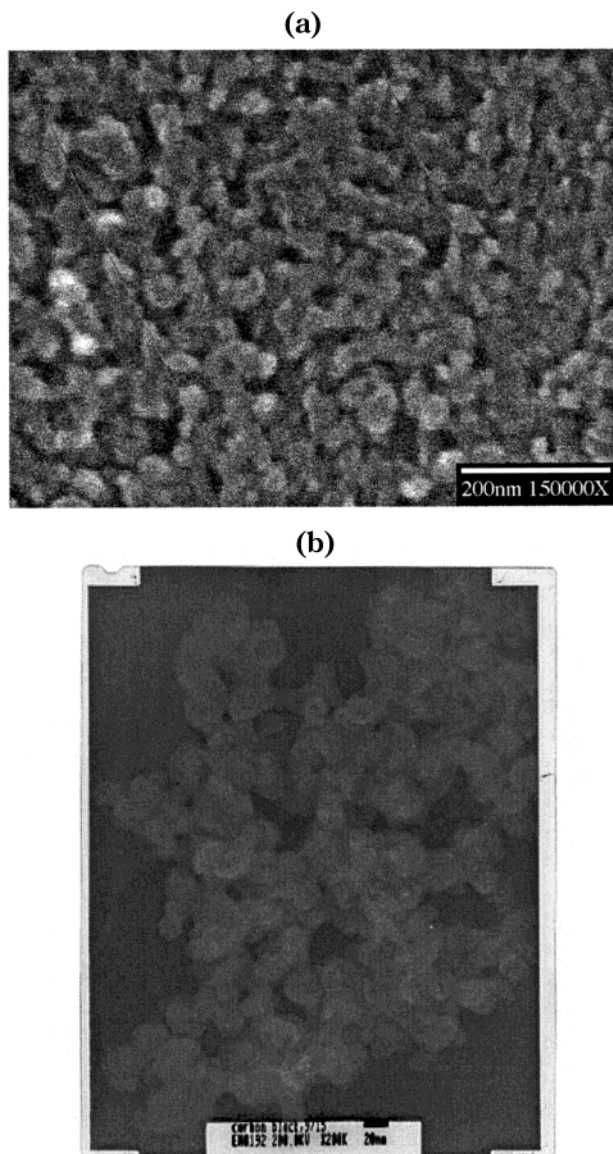


**Figure 8.** (a) SEM micrograph of dried carbon black powders. (b) TEM micrograph of CB particles. Particles with diameters of about 20–40 nm can be observed.

siloxane surfactants, the theoretical value of the C–O/CH<sub>2</sub> ratio is about 1.4. This condition again supports the evidence that the surface coverage by the siloxane surfactants is incomplete.

**SEM and TEM.** Figure 8a shows a SEM micrograph of dried carbon black powders. Discrete particle size cannot be estimated from this figure. Figure 8b shows a TEM micrograph of CB particles. The bar located below the figure indicates 20 nm. Particles with diameters of about 20–40 nm can be observed. These CB particles show fractal characteristics and aggregate to form clusters.

**Structure and Specific Surface Area of CB Particles.** To determine the adsorbed amount per surface area used in the adsorption isotherm, the surface area of CB particles should first be estimated. One way to estimate the surface area is to assume the diameter of the CB particles to be 100 nm (obtained by DLS as discussed below and as shown in Figure 11) and the density of the particle to be 2 g/cm<sup>3</sup>. Thus we obtain the specific surface area of CB to be 30 m<sup>2</sup>/g.

Since SANS data and TEM micrographs indicate that CB has fractal structure, we also estimate the surface

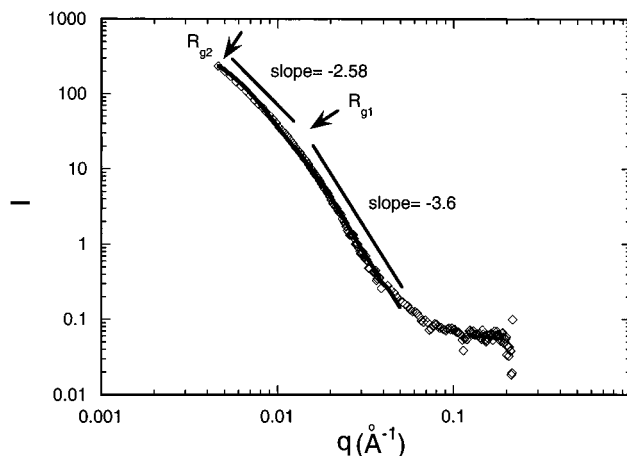


**Figure 9.** SANS intensity of CB particles at 87% H<sub>2</sub>O and 13% D<sub>2</sub>O (no surfactant is present). The CB particles show two structure levels. The higher  $q$  range originates from primary particles, and the lower  $q$  range from CB clusters. The data were fitted by the unified approach (see text for details), and  $R_{g1}$  and  $R_{g2}$  are the limits for the mass fractal.

area of the particles by eq 11. Figure 9 shows a typical SANS profile for CB particles (0.3%) dispersed in water with no surfactant added. The scattering patterns show two power-law regimes: At high  $q$ , a power law of  $-3.6$  is observed for the surface of the primary particle. At low  $q$ , a weak slope of  $-2.6$  corresponds to a mass-fractal regime. Gerspacher et al. found that the surface fractal dimension was nearly constant at a value of  $\sim 2.4$  for 15 different grades of CB.<sup>18</sup>

We can obtain eight parameters from fitting the scattering curve, that is,  $G_1$ ,  $B_1$ ,  $P_1$ ,  $R_{g1}$ ,  $G_2$ ,  $B_2$ ,  $R_{g2}$ , and  $d_f$ . The lower and upper limits of the mass fractal are characterized by  $R_{g1}$  and  $R_{g2}$ . The determination of degree of aggregation is somehow difficult, that is,  $G_2$  and  $R_{g2}$  are obscured due to the lack of information in the lower  $q$  region. We assume that  $R_{g2}$  is located at the limit of  $q$  ( $0.004 \text{ \AA}^{-1}$ ). Six clearly distinguishable parameters, the high- $q$  power-law prefactor  $B_1$ ,  $P_1$ ,  $R_{g1}$ ,  $G_1$ ,  $d_f$ , and low- $q$  power-law prefactor  $B_2$ , can be estimated, from which the four parameters of the model,  $G_1$ ,  $d_f$ ,  $R_{g1}$ , and  $z$ , can be obtained by fitting. The  $R_{g1}$  and  $R_{g2}$  values are 11.8 and 34.9 nm, respectively. The radius of spherical primary particles is  $R = (5/3)^{0.5} R_{g1} = 15.3 \text{ nm}$ , which is comparable to the size of the primary particles as seen in TEM (Figure 8b). Also, if we assume the aggregates form spherical particles then their radius is  $R = (5/3)^{0.5} R_{g2} = 45.0 \text{ nm}$ , which is very close to the 50 nm radius of the CB particles obtained by DLS (where diameter  $\sim 100 \text{ nm}$ ).

The surface area was estimated from eq 11 to be 283 m<sup>2</sup>/g with  $z = 11$  and  $Q = 6.84 \times 10^{-5} \text{ cm}^{-1} \text{ \AA}^{-3}$ . The volume of the primary particle that can be obtained from the high  $Q$  invariant by eq 10 ( $5.2 \times 10^7 \text{ \AA}^3$ ) and from a calculation using the radius of spherical primary particles ( $4/3\pi R^3 = 1.5 \times 10^8 \text{ \AA}^3$ ) shows some discrepancy. The reason lies in the deviation of the particles from spheres and in the uncertainty of  $R_{g2}$ . Since the TEM micrograph shows visual evidence of fractal structure and  $R = ((5/3)^{1/2} R_{g1} = 15.3 \text{ nm})$  is similar to the size of the CB primary particles shown in TEM and, moreover, since the particle shape does not differ much from spheres, we therefore take 283 m<sup>2</sup>/g as the specific area to use in the adsorption isotherm. Note, however, that this surface area may not be available in its entirety for the adsorption of the surfactant if the surfactant is hindered from accessing the inner surface of the fractal. The surfactant of interest here is macromolecular, so the surface area accessible to it will likely



**Table 3. Freundlich Isotherm Parameters, Langmuir Isotherm Parameters, and Surface Area Occupied by One Surfactant Molecule When Adsorbed on Various Particles**

particle	surfactant	Freundlich isotherm		Langmuir isotherm		
		$a$	$n$	$m^s$ (mg/m <sup>2</sup> )	$b$	$\sigma$ (nm <sup>2</sup> )
0.3% CB	siloxane	14.38	0.57	4.39	27.79	4.4
1.5% CB	siloxane	3.4	0.43	1.32	49.47	14.7
5% CB	siloxane	3.01	0.61	1.74	7.92	11.2

be closer to the 30 m<sup>2</sup>/g value (estimated for a compact sphere as described at the start of this section) than to the 283 m<sup>2</sup>/g value obtained from SANS. But since we do not have specific information on the surface area accessible to the surfactant, we report data based on 283 m<sup>2</sup>/g specific area and also indicate how the values would change if the area were 30 m<sup>2</sup>/g. Most CB particles have a specific surface area in the order of 100–900 m<sup>2</sup>/g<sup>12</sup> in agreement with the value obtained here from SANS.

**Adsorption Isotherm.** Figure 3 shows the initial total siloxane concentration versus the filtrate siloxane concentration at 0.3%, 1.5%, and 5% CB. The initial siloxane concentration is higher for higher CB concentrations in order to reach the same filtrate concentration for lower CB concentrations. Figure 4a shows adsorption isotherms of siloxane surfactants onto different concentrations of CB particles. The adsorbed amount increases as the CB concentration decreases from 5% to 0.3% since more surface areas are available at a higher CB concentration. We applied the Freundlich and Langmuir isotherm model to the experimental data. The Langmuir adsorption isotherm is theoretically derived and assumes one-to-one binding between the adsorbate and the binding site on the adsorbent. The Freundlich adsorption isotherm is experimentally derived and empirical. Real adsorption, however, is complex, and neither equation covers a wide range of adsorbate concentrations. The Freundlich equation can be described as

$$m_2^s = aC_f^{1/n} \quad (12)$$

where  $m_2^s$  is the adsorbed amount per unit surface area (mg/m<sup>2</sup>). The constant  $a$  gives a measure of the adsorbent capacity, and  $1/n$  of the intensity of adsorption.

The Langmuir isotherm can be determined by the following equation:

$$m_2^s = \frac{m^s b C_f}{1 + b C_f} \quad (13)$$

where  $b$  is the equilibrium constant and  $m^s$  is the maximum adsorbed amount per unit surface area (mg/m<sup>2</sup>).

Figure 4b shows the fitting of the Freundlich and Langmuir isotherms to the experimental data of 1.5% CB with different siloxane surfactant concentrations. The Langmuir isotherm equation provides a better fit to the experimental data at filtrate concentrations below 0.15% than the Freundlich isotherm equation. The Langmuir isotherm assumes monolayer adsorption; therefore, the siloxane surfactants follow monolayer adsorption at low filtrate concentrations. For 0.3% and 1.5% CB concentrations, the monolayer adsorption stops at about 0.15%, which is close to the cmc of the siloxane surfactant in water (0.05%). For 5% CB, the monolayer adsorption stops at 0.3%, implying more surfactants are needed in order to complete the monolayer adsorption. Above these filtrate concentrations, rapid increases in adsorbed amount occur and multilayers or other structures are apparently formed.

The structure of the adsorbed layer under these conditions will be explored later in this paper.

The Langmuir isotherm parameters can be determined graphically by the following equation (obtained from rearrangement of eq 13)

$$\frac{C_f}{m_2^s} = \frac{1}{m^s b} + \frac{C_f}{m^s}$$

A plot of  $C_f/m_2^s$  versus  $C_f$  should give a straight line of slope  $1/m^s$  and intercept  $1/m^s b$ .  $m^s$  is a measure of the adsorption capacity of the CB particles, and  $b$  (also called the binding constant) is a measure of the intensity of the adsorption. We obtained the parameters by fitting the data at conditions where they assume monolayer adsorption as discussed above.

The Langmuir isotherm parameters for 0.3%, 1.5%, and 5% CB in the monolayer adsorption region were determined in Figure 4c. The average surface area  $\sigma^0$  occupied by one surfactant molecule can be estimated by the Langmuir isotherm. The maximum adsorbed amount, equilibrium constants, and average surface area  $\sigma^0$  occupied by one surfactant molecule calculated from Figure 4c as well as the Freundlich isotherm equation constants  $a$  and  $n$  are listed in Table 3. The average surface area  $\sigma^0$  for one siloxane surfactant molecule is about 5–15 nm<sup>2</sup>. The Pluronic F108 PEO–PPO–PEO block copolymer, which has a higher molecular weight than this siloxane surfactant, has been found to have  $\sigma^0$  equal to 26 nm<sup>2</sup> on CB particles.<sup>37</sup> The plateau of the adsorption isotherm of 0.3% CB particles is 4.39 mg/m<sup>2</sup>, of 1.5% CB particles is 1.32 mg/m<sup>2</sup>, and of 5% CB particles is 1.74 mg/m<sup>2</sup>. If we use the surface area estimated by using the particle diameter we obtained from DLS, the plateau will be 9 times higher than these values.

From a comparison of the cmc values and the adsorbed amount onto CB particles of Pluronic P103, P104, P105, and F108 reported in the literature,<sup>36,37</sup> we find that the adsorption plateau region occurs at a concentration that is much smaller than the cmc of these surfactants, and the plateau was higher when EO chains were shorter. Pluronic F108 showed a much smaller plateau value than Pluronic P103, P104, and P105. The cmc of Pluronic F108 is 4.5% at 25 °C,<sup>36</sup> which is much higher than that of the siloxane surfactant we used in the current study. Its cmc (0.05%) is a little below the pseudoplateau in our system. Adsorption behavior similar to that in our system (i.e., as the filtrate concentration increases, the adsorbed amount suddenly increases) was observed by Shar et al.<sup>38</sup> who studied the adsorption isotherm of polystyrene and

(36) Alexandridis, P.; Holzwarth, J. F.; Hatton, T. A. Micellization of Poly(Ethylene Oxide)–Poly(Propylene Oxide)–Poly(Ethylene Oxide) Triblock Copolymers in Aqueous Solutions: Thermodynamics of Copolymer Association. *Macromolecules* **1994**, *27*, 2414–2424.

(37) Miano, F.; Bailey, A.; Luckham, P. F.; Tadros, Th. F. Adsorption of Poly(Ethylene Oxide)–Poly(Propylene Oxide) ABA Block Copolymers on CB and the Rheology of the Resulting Dispersions. *Colloids Surf.* **1992**, *69*, 9–16.

(38) Shar, J. A.; Cosgrove, T.; Obey, T. M.; Warne, M. R. Adsorption Studies of Diblock Copolymers at the Cyclohexane/CB Interface. *Langmuir* **1999**, *15*, 7688–7694.

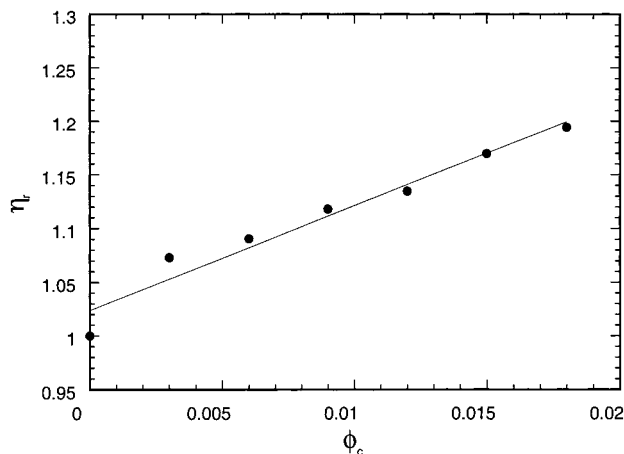


**Figure 10.** Relative viscosity of the aqueous CB suspension as a function of the particle volume fraction. The adsorbed layer thickness  $\Delta$  can be calculated from the slope by eq 2.

hydrogenated polyisoprene onto CB particles in a cyclohexane medium. In our case, it can be explained that the poor solvency of the siloxane in water leads to the complex formation (micelle or multilayer) at the interface and the adsorption isotherm is similar to the Brunauer–Emmett–Teller (BET) isotherm for a gas.<sup>42</sup>

$$m_2^s = \frac{m^s cx}{(1-x)(1+(c-1)x)} \quad \text{where } x = P/P^0$$

#### Viscometry

We considered that 0.15% is the filtrate siloxane concentration at the limit of monolayer adsorption and calculated the relative viscosity from eq 2 given in the Experimental Section. Figure 10 shows the relative viscosity of the CB aqueous suspension with adsorbed surfactant plotted versus the volume fraction of the CB core. From the slope of the data,  $2.5k$  is 9.7698, and thus the calculated  $k$  value is 3.908 and the resulting adsorbed layer thickness is 28.8 nm. We used the least-squares method to fit the data points; the curve did not pass through 1 as expected. This can be explained by the fact that the filtrate concentration for the same initial surfactant concentration (0.7%) is higher ( $>0.15\%$ ) at a low CB concentration than at a high CB concentration (see Figure 3 for the filtrate concentration at different amounts of CB particles) and would thus give a higher filtrate viscosity at a low CB concentration. Therefore, the relative viscosity should be lower at a low CB concentration, owing to the higher filtrate concentration, than the measured values (0.91 cSt). Thus the relative viscosity should be lower at a low CB concentration than what appeared in Figure 10. If we force the curve in Figure 10 to pass through 1 at the origin, the adsorbed layer thickness will increase by about 4 nm to reach a level of 32.8 nm.

#### Adsorbed Layer Thickness Determined by DLS

While SANS gives  $R_{g2}$  corresponding to the aggregate size as discussed above (34.9 nm), DLS also provides the

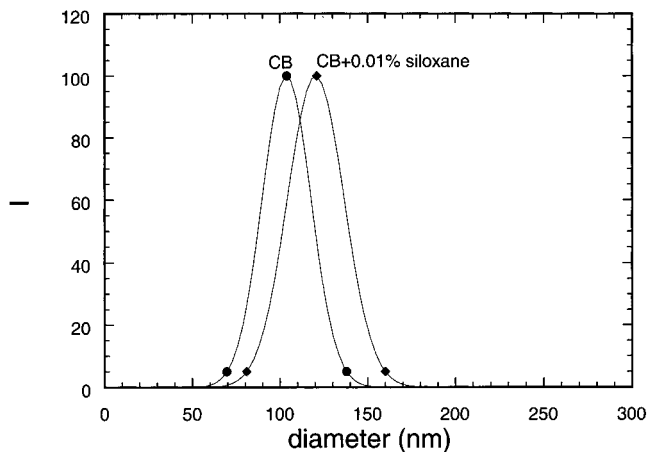


**Figure 11.** Diameter of CB particles ( $3.75 \times 10^{-4}\%$ ) with and without adsorbed siloxane surfactant obtained by DLS. The adsorbed layers from 0.01% siloxane surfactants (below cmc) increase the particle diameter from 103.8 to 120.5 nm.

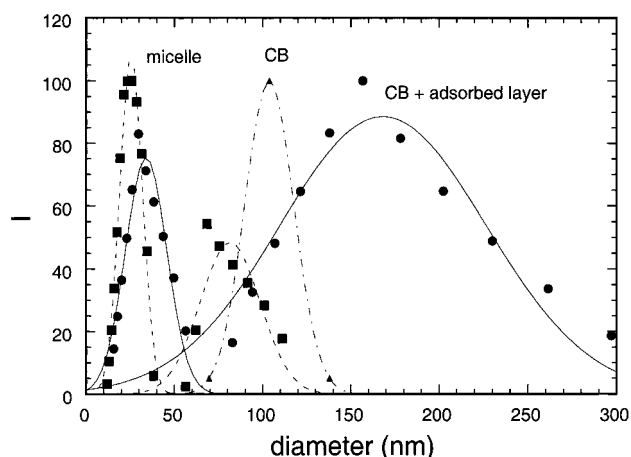


**Figure 12.** Dynamic light scattering data from  $3.75 \times 10^{-4}\%$  CB with 1% siloxane in water. The dashed–dotted line fits the size distribution of the CB particles. The dashed line fits the size distribution of the surfactant in the same solution without CB particles. The solid line fits the size distribution data of the particles with adsorbed siloxane surfactant. The lower size peak of the CB particles with adsorbed layers agrees well with the lower size peak of the surfactant solution, which corresponds to the micelle diameter of the surfactants. The mean hydrodynamic diameter (165.1 nm) of the higher peak in the case of CB + surfactant is larger than that of CB ( $\sim 100$  nm) in the absence of surfactant and than the higher peak of the surfactant solution ( $\sim 80$  nm).

information on the aggregate size. The CB particles have a hydrodynamic diameter of about 100 nm. The layers adsorbed from 0.01% siloxane surfactant (below cmc<sup>27</sup>) increase the particle diameter from 103.8 to 120.5 nm, as shown in Figure 11.

Figure 12 shows the size distribution of CB particles with an adsorbed layer of 1% siloxane surfactant in water. To better compare the siloxane surfactant coated CB particle size distribution to that of plain CB particles and to that of surfactant in solution when no CB particles were present, we present in the same plot distributions from three different systems: that of CB particles with adsorbed siloxane surfactant layers (solid lines), that of siloxane surfactant aqueous solution (dashed lines), and that of plain CB particles (dashed–dotted lines). The solid curves show two distributions. The lower peak of the siloxane surfactant coated CB size distribution is centered at around 30 nm and agrees well with the micelle diameter distribution (the lower distribution of the dashed lines).<sup>27</sup>

(39) Ozcan, O. Classification of Minerals According to Their Critical Surface Tension of Wetting Values. *Int. J. Miner. Process.* **1992**, *34*, 191–204.

(40) Evans, D. F.; Wennerstrom, H. *The Colloidal Domain*, 2nd ed.; Wiley-VCH: New York, 1999.

(41) van Oss, C. J. *Interfacial Forces in Aqueous Media*; Marcel Dekker: New York, 1994.

(42) Adamson, A. W.; Gast, A. P. *Physical Chemistry of Surfaces*, 6th ed.; John Wiley & Sons: New York, 1997.

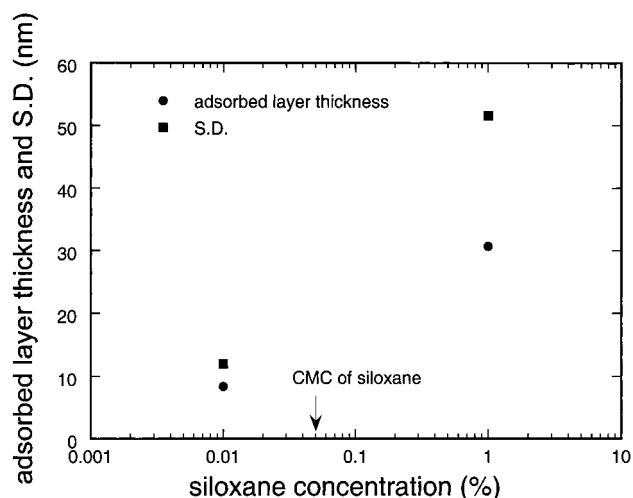


**Figure 13.** Effect of cmc on adsorbed layer thickness obtained by DLS. The arrow in this figure indicates the cmc of the siloxane surfactant. The adsorbed layer thickness increases from 8.4 to 30.7 nm as the siloxane concentration increases from 0.01%, passing through the cmc (0.05%), to 1%. The standard deviation of the particle size also increases from 12.0 to 51.6 nm as the siloxane concentration goes from below cmc to above cmc.

Note that the concentration conditions in these experiments are such that the micelle concentration (1%) is much higher than the CB particle concentration ( $3.75 \times 10^{-4}\%$ ). The higher peak of the siloxane surfactant coated CB particle size distribution shifts to a higher value (165.1 nm) than that resulting from the CB particles in the absence of surfactant ( $\sim 100$  nm) and than that of the siloxane aggregates (the higher distribution of the solid lines ( $\sim 80$  nm)). We choose the mean diameter of the higher distribution of the solid curves in Figure 12 as the diameter of the CB particles with an adsorbed surfactant layer.

The difference in the particle radius obtained with and without the presence of siloxane surfactant represents the thickness of the adsorbed surfactant layer. Figure 13 shows the cmc effect on the adsorbed layer thickness. The arrow in Figure 13 indicates the cmc of the siloxane surfactant. The adsorbed layer thickness increases from 8.4 to 30.7 nm as the siloxane surfactant concentration increases from 0.01%, passing through cmc (0.05%), to 1%. Below the cmc of the siloxane surfactant, the surfactant may not pack so tightly on the surface of the particles, and therefore the conformation of the polymer chains is not so extended and the adsorbed layer has a smaller thickness. The adsorbed layer structure above the cmc is discussed in detail in the following section. The standard deviation of the CB particle diameter distribution also increases from 12.0 to 51.6 nm as the concentration goes from below cmc to above cmc, which indicates a broadening of the size distribution of CB particles with adsorbed siloxane surfactant layers above the cmc. Sizes higher than 200 nm may result from aggregation of the CB particles due to the "bridging effect" of the surfactant.

**Structure of Adsorbed Layer.** Figure 14 shows the SANS patterns of 1% siloxane surfactant (above cmc) in 100%  $D_2O$  with and without 0.3% CB particles. These concentrations correspond to conditions well above the monolayer adsorption (see Figure 4). The siloxane concentration in solution is not too high to mask the CB particles at this concentration (as seen in Figure 3, the filtrate concentration of siloxane is about 0.2%, corresponding to its initial concentration of 1%); moreover, the unreacted polyethers present in solution have a molecular

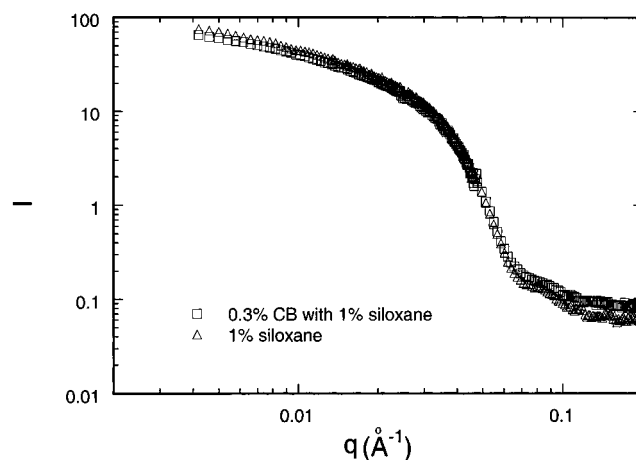


**Figure 14.** Scattering pattern of siloxane surfactants with and without the CB particles at 100%  $D_2O$ . The triangle symbols indicate the scattering from 1% siloxane surfactants in the absence of CB, and the square symbols indicate the scattering from 1% siloxane in the presence of CB (0.3%). The two curves coincide with each other, indicating that the presence of CB does not affect the siloxane micelle structure. Note that at 100%  $D_2O$  contrast the CB particles scatter very little.

weight that is too low and a PEO content that is too high to form any micelles. In the case of 100%  $D_2O$ , we matched the SLD of the solvent with the SLD of the CB particles and therefore the structure of CB was invisible, that is, we could only detect the structure of the siloxane surfactant. The triangle marks in Figure 14 indicate the scattering originating from siloxane surfactant in an aqueous solution (devoid of CB particles), while the square marks indicate the scattering from siloxane surfactant in an aqueous dispersion containing CB particles.

It is notable that the two curves coincide with each other. This suggests that the siloxane surfactant adsorbed on CB has the same structure as the siloxane in aqueous solution, that is, that of spherical micelles. The SANS pattern of the siloxane micelles in aqueous solution has been fitted by the hard-sphere model, and the micelle has a hard-sphere (core) diameter of 15 nm.<sup>27</sup> The micelle has a hydrodynamic diameter of about 26.4 nm as determined by DLS.<sup>28</sup> As discussed above, the CB particle radius measured by DLS increases by about 30.7 nm after the addition of siloxane surfactants, an increase that is very similar to the micelle hydrodynamic diameter. Both the SANS data of Figure 14 and the DLS data on the layer thickness (Figures 12 and 13) support the conclusion that the surfactant layer surrounding the CB particles is in the form of micelles. The SANS pattern obtained from a 0.3% CB aqueous dispersion containing 1% siloxane surfactant, at solvent conditions (13%  $D_2O$  + 87%  $H_2O$ ) where the siloxane surfactants are rendered invisible, is almost identical to the SANS pattern obtained from a 0.3% CB aqueous (13%  $D_2O$  + 87%  $H_2O$ ) dispersion without added surfactant, shown in Figure 9. This indicates that that the presence of the siloxane surfactant does not affect the structure of the CB particles.

From Figure 11, we can see that the diameter of the CB particles increases as the siloxane surfactant is adsorbed on the particles. The adsorbed layer thickness is 8.4 nm at 0.01% siloxane. We speculate that the structure of the adsorbed layer at this concentration is close to that of a monolayer (Figure 4a). When the siloxane concentration increases to 1%, the adsorbed layer takes the form of micelles. This can be attributed to a stronger affinity of the surfactant siloxane parts to each other than to the surface of the CB particles. Below cmc, the siloxane





**Figure 15.** Schematic of the adsorbed siloxane structure below and above the cmc (0.05%). At siloxane concentrations below the cmc, the adsorbed amount follows the Langmuir isotherm and the siloxane assumes monolayer adsorption. Above the cmc, the adsorbed layer thickness measured by viscometry and DLS and the structure determined by SANS both suggest that the adsorbed layer is in the form of micelles.

segments do not associate in solution (they do not form micelles) and thus prefer to adsorb to CB surfaces than to be exposed to water. Above the cmc, however, micelles form, and the siloxane segments prefer to associate with other siloxanes in the core of the micelles. The low affinity of siloxane to the CB particles may also be due to the lowering in the surface hydrophobicity, resulting from polar groups  $\text{COO}^-$  on the CB surface. While the siloxane molecules are organized in micelles, the siloxane micelles are not free in solution but tend to adsorb on the CB surface in a manner similar to that of high molecular weight polymers (the presence of siloxane surfactant on the CB surface has been established by XPS and also by the adsorption isotherm; adsorption of micelles on surfaces has been observed also in other systems). Figure 15 shows a schematic of the adsorbed siloxane layer structure on CB particles below cmc (monolayer) and above cmc (micelles).

### Conclusions

The dispersion stabilization of organic particles in aqueous media is of great importance for the preparation of waterborne coatings and inks of good quality. Carbon black, used as the pigment of black ink, is dispersed in an aqueous medium by a rake-type siloxane surfactant in this study. To understand the dispersion behavior, we first investigate the CB particle size, surface chemistry, and structure. We then determine the adsorption isotherm and adsorbed layer thickness and structure of the siloxane surfactants on CB particles. Such studies on the interactions between nanoparticles and polymeric surfactants provide fundamental information as well as practical data for use in designing formulations.

The chemical composition of CB particles obtained from XPS shows that a small portion of the particles has been oxidized to form  $\text{COO}^-$ . An increase in the silicone elements and ether groups after adsorbing the siloxane surfactants has been observed. This proves that the siloxane surfactants are adsorbed onto the CB particles. The oxygen and carbon contents on the surfaces of particles with adsorbed siloxane layers suggest incomplete coverage by the siloxane surfactant. TEM, SEM, DLS, and SANS were used to characterize the size and shape of the CB particles. The TEM micrographs show fractal structures of CB primary particles. These particles aggregate to form clusters. The diameter obtained by DLS is estimated to be 100 nm and should be the cluster size. From fitting SANS data with the unified approach, we can estimate the primary particle

radius (15.3 nm), which is in the same order as the size observed from TEM ( $\sim 20\text{--}40$  nm).

The adsorption isotherm for the rake-type siloxane surfactant, with the chemical structure  $\text{MD}_{70}\text{D}'_5\text{M}$  (M:  $\text{Me}_3\text{SiO}_{1/2}-$ ; D:  $-\text{Me}_2\text{SiO}-$ ; D':  $-\text{Me}(\text{R})\text{SiO}-$ ; R: polyether (PEO:900; PPO:300)), onto CB particles has been determined using a dialysis method, and a colorimetric method was developed to determine the siloxane concentration in water. The adsorption isotherm reaches a pseudoplateau region at the cmc and then increases at higher filtrate concentration at various CB concentrations. As the CB particle concentration increases, the adsorbed amount in the same filtrate concentration decreases. The Langmuir isotherm fits the adsorption behavior better than the Freundlich isotherm in low filtrate concentrations of siloxane surfactants onto CB particles, suggesting monolayer formation in lower filtrate concentrations.

Viscometry and dynamic light scattering provide complementary information on the adsorbed layer thickness of siloxane surfactants onto CB particles above cmc. The viscometric method allowed the determination of adsorbed layer thickness (28.8 nm) at higher CB concentrations. At a low surfactant concentration (below cmc) with CB particles, the CB particle radius obtained by DLS increases by about 10 nm, corresponding to monolayer adsorption. At a high surfactant concentration (above cmc), the CB aqueous suspension exhibits two size distributions; the lower peak corresponds to the siloxane surfactant micelles, and the upper peak corresponds to CB particles with adsorbed siloxane. The adsorbed layer thickness is  $\sim 30$  nm, comparable to the micelle hydrodynamic diameter obtained by DLS, 26 nm.

Two contrasts were used in SANS experiments carried out in aqueous CB dispersions containing siloxane surfactant. By matching the SLD of the aqueous solvent with that of CB, we can determine the structure of the siloxane surfactants; by matching the SLD of the solvent with that of siloxane, we can assess the structure of CB particles. SANS results suggest that the micelle structure is not altered by the addition of CB particles and that CB retains its structure following the addition of siloxane surfactants. The SANS data, together with viscometry and DLS which show similar adsorbed layer thickness very close to the micelle diameter, lead to the conclusion that the adsorbed layer has a structure in the form of spherical micelles.

**Acknowledgment.** We thank Xerox Foundation for partial funding of this work. We also thank the National Science Foundation (CTS-0124848/TSE) for partial support of this research. We acknowledge the support of the National Institute of Standards and Technology (NIST) in providing the neutron research facilities used in this work; this material is based upon activities supported by the National Science Foundation. We thank Dr. Jamie Schulz at NIST for valuable assistance with the SANS data acquisition. We thank Dr. Joachim Venzmer (Goldschmidt AG) for providing structure information on the siloxane surfactant used here. We thank Mr. Peter Bush (South Campus Instrumentation Center, University at Buffalo) for the acquisition of the XPS data.

LA011671T